Simultaneous Aerosol Mass Spectrometry and Chemical Ionisation Mass Spectrometry measurements during a biomass burning event in the UK: Insights into nitrate chemistry

Ernesto Reyes-Villegas[1], Michael Priestley[1], Yu-Chieh Ting[1], Sophie Haslett[1], Thomas Bannan[1], Michael Le breton[1*], Paul I. Williams[1,2], Asan Bacak[1], Michael J. Flynn[1], Hugh Coe[1], Carl Percival[1Δ], James D. Allan[1,2]

[1]School of Earth, Atmospheric and Environmental Sciences, The University of Manchester, Manchester, M13 9PL, UK
[2]National Centre for Atmospheric Science, The University of Manchester, Manchester, M13 9PL, UK
[*]Now at University of Gothenburg, 40530 Gothenburg, Sweden
[Δ]Now at Jet Propulsion Laboratory, 4800 Oak Grove Drive, Pasadena, CA 91109, USA

Correspondence to: Ernesto Reyes-Villegas (ernesto.reyesvillegas@manchester.ac.uk)

Abstract. Over the past decade, there has been an increasing interest in short-term events that negatively affect air quality such as bonfires and fireworks. High aerosol and gas concentrations generated from public bonfires/fireworks were measured in order to understand the night-time chemical processes and their atmospheric implications. Nitrate chemistry was observed during the bonfire night with nitrogen containing compounds in both gas and aerosol phase and further N_2O_5 and $ClNO_2$ concentrations, which depleted early next morning due to photolysis of NO_3 radicals, ceasing production. Particulate organic nitrate (PON) concentrations of 2.8 $\mu g.m^{-3}$ were estimated using the m/z 46:30 ratios from AMS measurements, according to previously published methods. ME-2 source apportionment was performed to determine organic aerosol concentrations from different sources after modifying the fragmentation table and it was possible to identify two PON factors representing primary (pPON_ME2) and secondary (sPON_ME2) contributions. A slight improvement in the agreement between the source apportionment of the AMS and a collocated AE-31 Aethalometer was observed after modifying the prescribed fragmentation in the AMS organic spectrum (the fragmentation table) to determine PON sources, which resulted in an $r^2 = 0.865$ between BBOA and b_{abs_470wb} compared to an $r^2 = 0.819$ obtained without the modification. Correlations between OA sources and measurements made using Time of Flight Chemical Ionization Mass Spectrometry with an iodide adduct ion were performed in order to determine possible gas tracers to be used in future ME-2 analyses to constrain solutions. During bonfire night, high correlations (r^2) were observed between BBOA and methacrylic acid (0.915), Acrylic acid (0.901), nitrous acid (0.864), propionic acid, (0.851) and Hydrogen cyanide (0.755). A series of oxygenated species, chlorine compounds as well as cresol showed good correlations with sPON_ME2 and the low volatility oxygenated organic aerosol (LVOOA) factor during an episode with low pollutant concentrations. Further analysis of pPON_ME2 and sPON_ME2 was performed in order to determine whether these PON sources absorb light near the UV region using an Aethalometer. This hypothesis was tested by doing multilinear regressions between b_{abs_470wb} and BBOA, sPON_ME2 and pPON_ME2. Our results suggest that sPON_ME2 does not absorb light at 470 nm while pPON_ME2 and LVOOA absorb light at 470 nm over that of black carbon. This may inform black carbon (BC) source apportionment studies from Aethalometer measurements, through investigation of the brown carbon contribution to b_{abs_470wb}.

1. Introduction.

Exposure to combustion aerosols has been associated with a range of negative health effects, in particular wood smoke aerosols have been shown to present respiratory and cardiovascular health effects (Naeher et al., 2007). Bonfires and fireworks are one of the main sporadic events with high emissions of atmospheric pollutants (Vassura et al., 2014;Joshi et al., 2016), even when these high emissions only last a couple of hours, high pollutant concentrations may instigate adverse

40   effects on human health (Moreno et al., 2007;Godri et al., 2010) and severely reduce visibility (Vecchi et al., 2008). Ravindra et al. (2003) found that the short-term exposure of air pollutants increases the likelihood of acute health effects.

Due to these adverse effects, different studies have been performed to analyse air pollution during important festivities around the world, for instance New Year's Eve celebrations (Drewnick et al., 2006;Zhang et al., 2010), the Lantern Festival in China (Wang et al., 2007) and Diwali festival in India (Pervez et al., 2016) as well as football matches such as during the

45   Bundesliga in Mainz Germany 2012 (Faber et al., 2013). In the UK, the bonfire night festivity takes place on November 5th to commemorate Guy Fawkes' unsuccessful attempt to destroy the Houses of Parliament in 1605 (Ainsworth, 1850). During this celebration, bonfires usually followed by fireworks, are lit domestically and on larger scale communally in public parks. Different studies have been carried out to assess the air pollution during bonfire night in the UK; for instance targeting the particle size distribution (Colbeck and Chung, 1996), investigating PM_{10} concentrations in different cities around the UK

50   during bonfires (Clark, 1997), measuring dioxins in ambient air in Oxford (Dyke et al., 1997); polycyclic aromatic hydrocarbons were measured in Lancaster, 2000 (Farrar et al., 2004) and potentially toxic elements were measured and their association to health risks was assessed in London (Hamad et al., 2015).

Receptor modelling has been widely used to determine OA sources in urban environments. However, it has been used in just a small number of studies with sporadic events of high pollutant concentrations. For instance Vecchi et al. (2008) was the

55   first to analyse measurements taken during firework displays using positive matrix factorisation (PMF). Tian et al. (2014) did a PMF analysis of $PM_{2.5}$ components, identifying five different sources: Crustal dust, coal combustion, secondary particles, vehicular exhaust and fireworks. In Riccione, Italy, Vassura et al. (2014) determined that levoglucosan, OC, PAHs, Al, and Pb, emitted from bonfires during St. Joseph's Eve, can be used as markers for bonfire emissions.

Particulate organic nitrates (PON) have been found to absorb light near the UV region (Mohr et al., 2013) and to present

60   potential toxicity affecting human health (Fernandez et al., 1992;Qingguo et al., 1995). PON also act as a NO_x reservoir in the night-time, releasing NO_x concentrations when the sun rises with the possibility of increasing O_3 production (Perring et al., 2013;Mao et al., 2013). PON are important components of organic aerosols; for instance Day et al. (2010), in measurements taken during winter at an urban location, found that PON concentrations accounted for up to 10% of organic matter. Kiendler-Scharr et al. (2016) concluded that, at a continental scale, PON represent 34% to 44% of aerosol nitrate.

65   Organic nitrates can be categorised, according to their origin, into two types; primary and secondary, primary organic nitrates are related to combustion sources (Zhang et al., 2016) such as fossil fuel (Day et al., 2010) and biomass burning emissions (Kitanovski et al., 2012;Mohr et al., 2013). Secondary organic nitrates are produced in the atmosphere, for example when NO_3 reacts with unsaturated hydrocarbons (Lee Ng et al., 2017). Nitrophenols, types of organic nitrates, are produced from reactions of phenols, both during the day reacting with $OH + NO_2$, and at night reacting with $NO_3 + NO_2$

70   (Harrison et al., 2005;Yuan et al., 2016).

The Aethalometer (Magee Scientific, USA) has been widely used to measure light absorbing carbon, proving to be a robust instrument capable to operate in a variety of environments and currently is being used at many different locations around the world. The European Environment Agency, in a technical report published in 2013 (EEA, 2013), states that there are at least 11 European countries using Aethalometers, for example; France, Italy, Slovenia, among others. The UK has a black carbon

75   (BC) network comprising 14 sites covering a wide range of monitoring sites (https://uk-air.defra.gov.uk/networks/network-info?view=ukbsn) and India started in 2016 a BC network with 16 Aethalometers (LASKAR et al., 2016). Commonly, Aethalometers have been used to separate sources of light-absorbing aerosols following Sandradewi et al. (2008). The approach separates absorption from traffic, predominately resulting from BC which absorbs light in the infrared region and from wood burning, which includes BC and absorbing organic matter that also absorbs near the ultraviolet region. The

80   Aethalometer model is based in the differences of aerosol absorption, using the absorption Ångström exponent, at specific

wavelength of light chosen to perform the model. Absorption Ångström exponent values range from 0.8-1.1 for traffic and 0.9-3.5 for wood burning (Zotter et al., 2017). It is known that Brown carbon (BrC) is organic matter capable of absorbing light near the UV region (Bones et al., 2010;Saleh et al., 2014) and that PON is a potential contributor to BrC (Mohr et al., 2013). However, the mechanistic behaviour that links this behaviour to wood burning has not completely been resolved and

85   there may be other sources such as secondary organic aerosols that can absorb near the UV region.

Here we present analysis performed on data collected during bonfire night celebrations in Manchester UK (29th October to 10th November 2014) using a cToF-AMS and a HR-ToF-CIMS along with other instruments to measure both aerosols and gaseous pollutants with the aim of understanding the night-time chemical processes and their atmospheric implications. Very high concentrations of pollutants occurred as a result of the meteorological conditions, which presented a good opportunity

90   to investigate the detailed phenomenon as a case study, particularly the possibility to determine PON concentrations, their nature and interaction with Aethalometer measurements.

2. Methods

2.1 Site and instrumentation

Online measurements of aerosols and gases were taken from ambient air, between 29th October and 10th November 2014, at a

95   rooftop location at the University of Manchester [53.467˚ N, 2.232˚ W], in order to quantify atmospheric pollution during the bonfire night event on and around 5th November. Figure S1 shows a map with the location of the monitoring site and nine public parks where bonfire/fireworks were displayed around greater Manchester. This is the same dataset presented by Liu et al. (2017).

A compact time of flight Aerosol Mass Spectrometer (cToF-AMS, here after AMS) was used to perform 5-minute

100   measurements of organic aerosols (OA), sulfate (SO_4^{2-}), nitrate (NO_3^-), ammonium ($NH4^+$) and chloride (Cl^-) (Drewnick et al., 2005). A High Resolution Time of Flight Chemical Ionization Mass Spectrometer (HR-ToF-CIMS, here after CIMS) was used to measure gas phase concentrations, using iodide as a reagent (Lee et al., 2014). The methodology to calculate gas phase concentrations from CIMS measurements are been described by Priestley et al. (In preparation). An Aethalometer, model AE31 (Magee Scientific), measured light absorption at seven wavelengths (370, 450, 571, 615, 660, 880 and 950 nm)

105   and a Multi Angle Absorption Photometer (MAAP; Thermo Model 5012), expressed as a BC concentration using the factory default settings (Petzold et al., 2002). NO_x, CO, O_3 and meteorology data were downloaded from Whitworth observatory (http://www.cas.manchester.ac.uk/restools/whitworth/data/), which were measured at the same location. From 31st October to 10th November, a catalytic stripper was attached to the AMS, switching every 30 minutes between direct measurements and through the catalytic stripper. These measurements were performed as part of a different experiment (Liu

110   et al., 2017). In the present study we used the AMS data from the direct measurements only, aerosol and gas data from other instruments were averaged to AMS sampling times.

2.2 Source apportionment

2.2.1 Aethalometer model

The aerosol light absorption depends on the wavelength and may be used to apportion BC from traffic and wood burning

115   from Aethalometer measurements as proposed by (Sandradewi et al., 2008). The absorption coefficients (b_{abs}) are related to the wavelengths at which the absorptions are measured (λ) and Ångström absorption exponents (α) with the relationship: $b_{abs} \propto \lambda^{\alpha i}$, thus the following equations can be solved:

$$\frac{b_{abs\_470tr}}{b_{abs\_950tr}} = \left(\frac{470}{950}\right)^{-\alpha_{tr}} \tag{1}$$

120 $$\frac{b_{abs\_470wb}}{b_{abs\_950wb}} = \left(\frac{470}{950}\right)^{-\alpha_{wb}} \tag{2}$$

$$b_{abs}(470_{nm}) = b_{abs\_470tr} + b_{abs\_470wb} \tag{3}$$

$$b_{abs}(950_{nm}) = b_{abs\_950tr} + b_{abs\_950wb} \tag{4}$$

125 Here, it is possible to calculate the wood burning (wb) and traffic (tr) contributions to BC at 470 and 950 nanometres (nm) as used in previous studies (Crilley et al., 2015;Harrison et al., 2012). Wavelengths 470 and 950 nm were chosen as Zotter et al. (2017) determined that using this pair of wavelength resulted in less residuals compared when using the pair of wavelengths 470-880, and 370-880 nm. Before the Aethalometer model was applied, the absorption coefficients (b_{abs}) needed to be corrected following Weingartner et al. (2003) as attenuation is affected by scattering and loading variations. The following
130 parameters were calculated: multiple scattering constant C = 3.16 and filter loading factors (f) of 1.49 and 1.28 for the wavelengths 470 and 950 nm respectively. Refer to section S3 in supplement for detailed information.

2.2.2 Multilinear engine 2 (ME-2)

Multilinear engine 2 (Paatero, 1999) is a multivariate solver used to determine factors governing the behaviour of a two dimensional data matrix, which then can be interpreted as pollutant sources. ME-2 uses the same data model as positive
135 matrix factorisation, which is also a receptor model that performs factorisation by using a weighted least squares approach (Paatero and Tapper, 1994).

In order to explore the solution space, ME-2 is capable of using information from previous studies, for example pollutant time series or mass spectra, as inputs to the model (named target time series and target profiles respectively) to constrain the runs. These constraints are performed using the a-value approach, to determine the extent to which the output is allowed to
140 vary. For example, by using an a-value of 0.1 to a specific source, the user is allowing the output to vary 10% from the input. For more details refer to Canonaco et al. (2013).

In this study, ME-2 and PMF were used through the source finder interface, SoFi version 4.8 (Canonaco et al., 2013) to identify OA sources using the suggestions made by Crippa et al. (2014) and the strategy proposed by Reyes-Villegas et al. (2016). ME-2 was performed using mass spectra (BBOA, HOA and COA) from two different studies as target profiles (TP)
145 to constrain the runs; London (Young et al., 2015) and Paris (Crippa et al., 2013), Fig. S6 explains the labelling used to identify the different runs. Factorisation struggles to separate two or more sources if they are highly correlated, for example during stagnant conditions due to low temperatures and wind speed, which was the case during the bonfire night 2014. The pollutants were well-mixed, making it difficult to separate the sources. Thus, four tests were performed, comparing 19 runs per test, using different time sets in order to identify the best way to perform source apportionment:

150 - Test 1 performs factorisation on all the dataset.
- Test 2 involves factorising the period before and after bonfire night and using mass spectra from this analysis as TP to factorise the bonfire night period.
- Test 3 involves factorising the bonfire night event and using mass spectra from this analysis as TP as applied to the complete dataset.
155 - Test 4 involves factorising the period before and after bonfire night and using mass spectra from this analysis as TP to factorise the full dataset.

3. Results

3.1 Meteorology and pollutant overview

160   During bonfire night festivities on November 5th, a temperature of 4 ˚C and wind speed of 1.5 m.s⁻¹ were observed (Fig. 1.a), causing stagnant conditions which facilitated pollutant accumulation. Looking at the time series for the whole sampling time (Fig. 1.b), it was possible to observe four separate events with different pollutant behaviour (marked with coloured lines over the x-axis in Fig. 1), driven by different meteorological conditions: one episode had high secondary concentrations (HSC, yellow line) from October 30th to November 1st, which experienced a relatively high temperature of 17-20 ˚C; one period of

165   low pollutant concentrations (LC, grey line) from November 1st - 3rd was observed when continental air masses were present; Bonfire night (bfo, blue line), with a temperature of 4 ˚C; and a winter-like episode (WL, purple line) from November 8th - 10th, with temperatures of 5-6 ˚C and high primary pollutant concentrations.

Aerosol concentrations during bonfire night were particularly high (Fig. 1.c), with the highest peak concentrations of 65.0, 19.0, 6.8, 6.0, 5.9 and 3.2 µg.m⁻³ for OA, BC, SO_4, Cl, NH_4 and NO_3 respectively measured around 20:30 hrs on November

170   5th. It is worth noting how high these concentrations are compared to concentrations before and after bonfire night (Fig. 1.b) where aerosol concentrations ranged from 0.5 – 7.0 µg.m⁻³. Measured PM_1 concentrations (sum of BC, organic and inorganic aerosols) of 115 µg.m⁻³ (Fig. 1.c) were observed during bonfire night.

Looking at the daily concentrations (Fig. 1.d), it is possible to observe PM_1 daily concentrations of 25 µg.m⁻³ on bonfire night compared to the low concentrations observed between November 1st – 2nd with concentrations ranging between 3-4

175   µg.m⁻³. The impact of the emissions during bonfire night is present even during the next day with PM_1 concentrations of 14 µg.m⁻³.

Gas phase pollutants were measured at the Whitworth observatory. Figure 2 shows high SO_2, CO and NO_x concentrations during bonfire night; these primary pollutants are well known to be combustion related pollutants. The high SO_2 concentrations during bonfire night are expected as solid fuels such as wood emit SO_2 when burned. This can also explain

180   the SO_2 peak in the night of November 10th - 11th when SO_2 concentrations may be related to solid fuels used for domestic heating as a result of the low temperatures (6 ˚C). CO and NO were present at higher concentrations during bonfire night compared to previous days with concentrations reaching 1600 ppb (CO) 99 ppb (NO) during bonfire night compared to November 1st with concentrations of 230 ppb of CO and 16 ppb of NO.

3.2 Bonfire night analysis

185   #### 3.2.1 Traffic and wood burning contributions to BC

OA concentrations started increasing at 19:30 hrs while BC concentrations started increasing two hours earlier around 17:00 hrs (Fig. 1.c). This rise in BC concentrations may be due to bonfire emissions, although they may also be related to traffic emissions; thus the Aethalometer model was used to identify both traffic and wood burning contributions to BC.

Once, b_{abs} are corrected, equations shown in section 2.2.2 are used to apply the Aethalometer model, with Ångström

190   absorption exponents (α) of 1.0 for traffic ($α_{tr}$), using the wavelength 470 nm, and 2.0 for wood burning ($α_{wb}$) using the wavelength 950 nm, to determine traffic and wood burning contributions. Figure 3 shows the absorption coefficients for wood burning b_{abs_470wb} (blue) and traffic b_{abs_950tr} (red), both increasing around 17:00-18:00 hrs to values lower than 100 Mm⁻¹ while b_{abs}, indicating contributions from wood burning and traffic during this period. It is when the majority of bonfire events are taking place, around 20:00, when b_{abs_470wb} shows the greatest increase, with values reaching 480 Mm⁻¹ compared

195   to 150 Mm⁻¹ for b_{abs_950tr}.

3.2.2 Particulate Organic nitrate (PON)

200   Currently, there is not a direct technique to measure on-line integrated PON concentrations; however, it is possible to estimate PON concentrations from AMS measurements using the m/z 46:30 ratios (Farmer et al., 2010), where NO_2^+ corresponds to m/z 46 and NO^+ to m/z 30. While we are assuming that the signal at m/z 30 corresponds to NO^+ from NH_4NO_3 and PON, it is possible to have interference of mineral nitrates (e.g. KNO_3 and $NaNO_3$) and organic CH_2O^+. However, mineral nitrate salts tend to be large particles (Allan et al., 2006;Chakraborty et al., 2016) and also have low

205   vaporisation efficiency (Drewnick et al., 2015), which makes it unlikely to be measured by the AMS in large quantities. The possible interference of CH_2O^+ will be explored in section 3.4.1. This event during bonfire night 2014, with high pollutant concentrations, provided the opportunity to identify the presence of PON. Inorganic nitrate from NH_4NO_3 has been detected at m/z 46:30 ratios between 0.33 and 0.5 (Alfarra et al., 2006) and of 0.37 (Fry et al., 2009), although each instrument-specific ratio is determined during routine calibrations. PON has been identified with m/z 46:30 ratios of 0.07-0.10 (Hao et

210   al., 2014) and 0.17-0.26 (Sato et al., 2010). In this study, m/z 46:30 ratios of 0.11-0.18 were observed during bonfire night (Fig. 4), confirming the presence of PON during this event. In this study, PON concentrations were calculated using the equations proposed by Farmer et al. (2010) and the considerations identified by Kiendler-Scharr et al. (2016) (Supplement S5). Figure 4 shows PON concentrations of up to 2.8 µg.m^{-3} during bonfire night, which are over the detection limit of 0.1 µg.m^{-3} reported by Bruns et al. (2010). PON concentrations are considered high compared to previous studies with

215   concentrations between 0.03 – 1.2 µg.m^{-3}, from a wide variety of sites across Europe (Kiendler-Scharr et al., 2016), while high PON concentrations of 4.2 µg.m^{-3} were observed during a biomass burning period in Beijing, China (Zhang et al., 2016).

3.3 OA source apportionment

This event with high pollutant concentrations during bonfire night gave the opportunity to test ME-2 factorisation tool under

220   these conditions and determine the best way to perform OA source apportionment. Four different tests were performed, refer to section S6 in supplementary material for detailed information. From the four tests performed, test 2 is the test that better deconvolved the OA factors. Test 2 involved two steps: in step a, PMF/ME-2 were run for the period before and after the bonfire night (named as not bonfire period, nbf). In Step b, mass spectra from the solution identified in step a were used as TP, to analyse the bonfire-only (bfo) event (05-Nov 17:00 hrs – 06-Nov 12:00 hrs). Finally, both solutions (nbf and bfo)

225   were merged for further analysis (Fig. 5.d).

Figure 5.c shows mass spectra of the two chosen solutions; five sources were identified during nbf period: BBOA, HOA, COA, SVOOA and LVOOA. In the case of the bfo period six different sources were identified: BBOA, HOA, COA, factor4 which seems to be a mixed factor with a peak at m/z43 (characteristic of SVOOA) and peaks at m/z_55 and m/z 57 (characteristic of HOA), LVOOA and BBOA_1. This BBOA_1 source appears to be a mixed factor between LVOOA (peaks

230   at m/z28 and mz44) and BBOA (peak at m/z60).

3.3.1 Source apportionment to determine PON nature

PON may exhibit covariance with other types of OA, thus their inclusion in the analysis may give a more complete factorisation and highlight their co-emission with other OA types. Therefore, a different experiment was designed by modifying the fragmentation table, through the ToF-AMS analysis toolkit 1.56, in order to identify a PON source. The

235   fragmentation table contains the different chemical species measured by the AMS, with each row representing m/z for

specific species and where the user can define peaks that exist in each species' partial mass spectrum and their dependency on other peaks (Allan et al., 2004). The following steps were performed to modify the fragmentation table:

- Time series of the ratio PON:mz30 were calculated with the equation: PON:mz30 = PON/mz30. Where PON is calculated from m/z 46:30 ratios (Farmer et al., 2010) and mz30 is the raw signal at m/z=30 measured by the AMS.
240   Refer to section S4 for PON estimation.

- In the FragPanel, the column frag_Organic, m/z 30 was multiplied by ratio_PON_30 time series.

- PMF inputs are generated to be used in SoFi software.

Here two tests were performed; source apportionment to all data set (Test 1_ON) and source apportionment to nbf period with subsequent source apportionment to bfo period (Test 2_ON). Test 2_ON resulted in being the test that better separated
245 OA factors. Figure 6.c shows mass spectra of the two chosen solutions, five sources were identified during nbf period: BBOA_2, HOA, COA, secondary particulate organic nitrate (sPON_ME2), and LVOOA. In the case of the bfo period six different sources were identified: BBOA_2, HOA, COA, LVOOA and two factors with peaks at m/z30, which is related to PON. These two PON factors may have different sources; one may be secondary (sPON_ME2) and the other primary (pPON_ME2), this possibility will be further explored in section 4.4.

250 The possible interference of CH_2O^+ at m/z 30 is unlikely as the signal of CH_2O^+ at m/z 30 is typically low compared with other organic peaks, while Fig. 6.c shows m/z 30 to be the predominant peak for both sPON_ME2 and pPON_ME2 factors. Section 3.4 shows the importance of performing OA source apportionment using different approaches in order to identify the best way to deconvolve OA sources. The techniques developed here may be of use for future case study analyses.

4. Discussion

255 **4.1 PON factor and improvement to source apportionment**

As seen in section 3.5, two different exercises of OA source apportionment were performed, one modifying the fragmentation table to determine a PON factor and the another one without modifying it. In both studies, test 2 proved to be the one that better deconvolved OA sources after doing the comparsions in section S6 in the supplement. This means that, in general, the best way to perform source apportionment during a special event with high concentrations is to first analyse the
260 period before and after bonfire night (nbf) with further analysis of the bonfire night period (bfo), using BBOA, HOA and COA mass spectra from the solution chosen in the nbf analysis as TP. When first analysing the period before and after the bonfire, source apportionment is performed on OA concentrations without significant variations and the OA sources identified may be representative of typical OA sources from Manchester during this sampling period. Furthermore, when using the mass spectra from these OA sources to analyse the bonfire night event, it is possible to separate the typical
265 "background" concentrations from the sources present during this special event.

It is worth noting that COA and HOA are present in high concentrations during the bonfire night event in both analyses (Fig. 5 and 6). High concentrations of these sources could expected as these (traffic and cooking activities) increase before and after the main bonfire events and the night represented a very strong inversion (which will trap all pollutants), but given the high concentrations experienced during the event and known variability for biomass burning emissions, the 'model error'
270 and thus rotational freedom is likely to be substantial. The result is that these two factors could contain indeterminate contributions from minor variabilities within the biomass burning profile and therefore must be interpreted with caution. But

it should be noted that the mass spectra of COA and HOA have their characteristic peaks at m/z 55 and m/z 57 and a higher m/z 57 for HOA than for COA, showing there is no apparent mass spectral 'mixing' with BBOA.

b_{abs_470wb} has the same source as BBOA, thus the correlation between these two can be used to evaluate the effectiveness of
275   BBOA deconvolution from OA concentrations (Frohlich et al., 2015;Visser et al., 2015). Here r^2 values are calculated for the bfo period between b_{abs_470wb} and the two BBOA's obtained in section 3.4; BBOA, obtained without modifying the fragmentation table and BBOA_2 obtained after modifying the fragmentation table to identify a PON factor. A higher correlation between b_{abs_470wb} and BBOA_2 was observed with $r^2 = 0.880$ compared to $r^2 = 0.839$ for b_{abs_470wb} and BBOA. This improvement on the BBOA_2 is explained by the fact that the PON factor may be mixed with BBOA and when both
280   sources are separated a higher correlation between BBOA_2 and b_{abs_470wb} is present.

4.2 PON Primary/secondary.

PON concentrations, obtained from the m/z ratios 46:30 (blue line in Fig. 7) have similar trend as BBOA, both increasing at the same time, suggesting a primary origin, but after 22:00 hrs, when BBOA concentrations drop, PON concentrations remain present with a slow decrease and maintaining low concentrations when BBOA concentrations were not present any
285   more. This suggests the hypothesis that there might not be only one type of PON, and it could be divided into primary and secondary organic nitrate as reported in previous studies performed in western Europe (Kiendler-Scharr et al., 2016;Mohr et al., 2013).

Using this working hypothesis, primary and secondary PON concentrations were estimated using the slope between PON and BBOA, calculated from 18:00 – 12:00 hrs, time when the main bonfire night event took place (Fig. S12). PON
290   concentrations were multiplied by this slope in order to calculate the primary organic nitrate (pPON) and secondary organic nitrate concentrations were calculated as: sPON = PON - pPON. Figure 7 shows the time series of this estimation where pPON reaches 2.5 ugm-3 and sPON with concentrations of 0.5 μg.m^{-3}.

A similar behaviour with two different PON sources was observed in the source apportionment analysis performed in section 3.4.1, where it was possible to separate two factors with a peak at m/z 30, characteristic of PON. Figure 8 shows that around
295   02:00 hrs, concentrations of the pPON started to decrease (green line) while sPON concentrations (grey line) increased. This analysis shows the presence of two different types of PON, pPON is primarily emitted along with BBOA concentrations with the further presence of a different PON, considered to be secondary, due to its increase when primary pollutants start to decrease. It is worth noticing that the increase of sPON takes places around 2:00 hrs, a period when NO concentrations started decreasing and CIMS-measured N_2O_5 and $ClNO_2$ started to increase suggesting that nitrate radical chemistry was
300   occurring (Fig. 9), which is possibly the source of the sPON, although the exact mechanism can only be speculated on.

This nitrogen chemistry process can be observed also in the gas phase, during the day, the main oxidants are O_3 and OH while the nitrate radical is unable to participate in daytime chemistry due to being rapidly photolyzed or reacting with NO to produce NO_2, (Ayres et al., 2015). Nitrate chemistry at night is important as nitrate radicals can be the main oxidants in polluted nocturnal environments away from enhanced NO and can create reservoirs and sinks of NO_x. The main NO_x
305   removal at night is via the uptake of dinitrogen pentoxide (N_2O_5) into aerosols, as at night N_2O_5 is formed from NO_3 and NO_2. In the presence of chloride in the particle phase (e.g. in sea salt particles), N_2O_5 reacts to produce nitryl chloride ($ClNO_2$). In the morning, following overnight accumulation of $ClNO_2$, photochemical reactions take place to produce Cl and NO_2. N_2O_5 and $ClNO_2$ processing an iteractions with nitrate chemistry has been previously studied in the UK (Le Breton et al., 2014a;Bannan et al., 2015). Figure 9 shows N_2O_5, $ClNO_2$ and O_3 concentrations increasing when NO and NO_2
310   concentrations decrease. All these processes may facilitate the sPON production at night. N_2O_5 concentrations reduce quickly after the sun rises, around 08:00 hours, while $ClNO_2$ concentrations decrease at a slower rate, with the lowest

concentrations observed around 13:00 hours. Along with NO_3 chemistry, it was possible to observe other nitrogen containing gases during bonfire night using the CIMS such as hydrogen cyanide (HCN) and Nitrous acid (HONO), which have been found to be emitted from fires (Le Breton et al., 2013;Wang et al., 2015). High HONO concentrations at night are important

315 during next morning when HONO reacts to produce OH and NO which impacts both the OH budget and NO_x concentrations early next morning.

4.3 OA factors and CIMS correlation

Analysing the CIMS measurements and comparing them with the OA factors, it may be possible to identify gas markers that can be used as inputs (target time series) to constrain solutions in future ME-2 analyses or as proxies when AMS data is not

320 available. A linear regression was performed between the OA sources determined in section 3.4.1 and CIMS peaks that have been considered positively identified (Priestley et al., in preparation), performing a coefficient of determination (r^2) analysis for the complete dataset (ALL), and the periods HSC, LC, bfo and WL. During the event HSC, none of the OA sources showed an r^2 higher than 0.6. HOA did not have an r^2 higher than 0.6 with any of the different events analysed. There were no specific markers identified for COA, while COA showed r^2 values higher than 0.6 for bfo period, these r^2's were observed

325 also with BBOA even with higher values. Table 1 shows the r^2 values, higher or equal to 0.6, obtained in this analysis. It is worth noting that r^2 values in ALL period seem to be influenced by the bfo event; this is the case for BBOA, COA and LVOOA which show similar r^2 values in both events. Thus, the analysis will be explained only in the individual events: bfo LC, and WL.

As expected, during bfo, BBOA is the OA source that shows the highest number of correlations during bonfire night. During

330 bfo episode, high correlations (r^2) were observed with BBOA and methacrylic acid (0.915), Acrylic acid (0.901), nitrous acid (0.864), propionic acid, (0.851) and Hydrogen cyanide (0.755), which have been previously determined as biomass burning tracers (Veres et al., 2010;Le Breton et al., 2013). Formic acid presented a high correlation (r2=0.858) with BBOA during bonfire night, however this value drops to 0.515 for all the dataset, which suggests formic acid during bonfire night is mainly primary while formic acid concentrations measured for the whole dataset may be related to primary and secondary sources.

335 This agrees with Le Breton et al. (2014b) who explored both primary and secondary origins of formic acid.

During the bfo period, LVOOA did not show a characteristic gas marker as all the r^2 values were also observed with BBOA. This suggests two hypotheses, that the LVOOA was mixed with BBOA, in the form of humic-like material (Paglione et al., 2014), which cannot be differentiated from secondary OA in the mass spectra (Fig. 6.c), or it could also be that secondary LVOOA may actually be present at the same time as BBOA concentrations, as it has been observed that during high relative

340 humidity and low temperature enhanced partitioning of semi-volatile material to the particle phase occurs. Moreover, due to the high aerosol concentration present during the bonfire night, there is more surface available for gases to be condensed and more particulate bulk to absorb into, thus it could be speculated that there would be high secondary aerosol concentrations. However, this is deemed unlikely, as there is unlikely to be much gas phase oxidation occurring in the presence of such high NO concentrations, which will remove ozone and nitrate radicals, the main source of oxidants at night.

345 In the case of organic nitrates, during the bfo period, sPON_ME2 did not show any correlation with gases, while pPON_ME2 showed r^2 values with CO and SO_2 with r^2 values of 0.78 and 0.72 respectively, which are typical primary pollutants related to combustion processes. High r^2 values were also observed during LC episode between $ClNO_3$ and LVOOA and sPON (0.66 and 0.60 respectively) proving their secondary origin.

This analysis showed a series of gases with high correlations with OA factors. Correlations changed within different periods,

350 with the bfo and WL periods being those with higher correlations. During bfo, BBOA and pPON showed to be related to primary emissions and during LC period LVOOA and sPON_ME2 showed to be secondary in nature.

4.4 PON and its relationship with b_{abs_470wb} and BBOA

Organic nitrates, originating from biomass burning, have been previously found to absorb light near the UV region (Jacobson, 1999;Flowers et al., 2010;Mohr et al., 2013). However, there is still a question of whether this absorption is due to primary or secondary PON. Here, the relationship between b_{abs_470wb} and PON and BBOA will be analysed to determine if sPON absorbs at 470 Mm^{-1}, which would interfere with Aethalometer measurements.

In order to quantitatively determine any contribution from organic nitrates to the Aethalometer data products, a multilinear regression (MLR) analysis was performed on the complete dataset dataset (ALL), and the events HSC, LC, bfo and WL. This analysis was done in three ways: MLR 1 with BBOA from OA source apportionment without modifying the FragPanel and PON from m/z 46:30 analysis; MLR 2 with BBOA_2 from OA source apportionment after modifying the FragPanel and PON from 46:30 analysis; MLR 3 with with BBOA_2 and PON_ME2 from OA source apportionment after modifying the FragPanel (Table 2). The following bilinear regression was used:

$$b_{abs\_470wb} = A + B*x1 + C*x2 \qquad (6)$$

where x1=BBOA [ugm-3], x2 = PON [ugm-3]. When the parameter "D" is used it means a trilinear regression was performed.

Table 2 shows the MLR outputs where; A represents the background, B, C and D represent the partial slope between b_{abs_470wb} and the respective organic aerosol. B/C represents the ratio between B and C partial slopes, with the following considerations: if B/C < 1 then, there is a higher contribution of organic nitrates to b_{abs_470wb}; if B/C > 1 then, there is a higher contribution of BBOA to b_{abs_470wb}. Looking at the coefficient of determination of the multilinear regression (r^2_MLR) for the three MLR analyses, it is possible to observe that HSC and LC periods present low r^2_MLR values ranging from 0.064 and 0.418, while bfo and WL events have high correlations with values between 0.760 and 0.910, which shows that is during high primary OA emissions are present when a high correlation between babs and BBOA and PON is observeed.

These high r^2 values, particularly during the bfo event which presented the highest r^2 (0.910), are consistent with previous studies that found organic nitrates absorb at short wavelengths; Mohr et al. (2013) identified correlation values of 0.65 between nitrophenols and babs$_{370wb}$. Teich et al. (2017), in a recent study from offline filters, determined nitrated aerosol concentrations with further analysis of the light absorption of aqueous filter extracts (babs$_{370}$), identified r^2 values between babs$_{370}$ and nitrated aerosol concentrations of 0.67 to 0.74 depending on acidic or alkaline conditions respectively.

In MLR 3, it is possible to observe that, during bfo period, the main contribution to b_{abs_470wb} is attributed to both BBOA_2 (16.657) and pPON_ME2 (7.357) while babs:sPON_ME-2 values were zero, with an optimum r^2 of 0.910. This lack of correlation between babs and sPON is observed in the linear regression babs:sPON_ME2 with an r^2 of 0.188. These results show that while there is evidence of pPON_ME2 absorbing at 470 nm, with a partial slope of 16.657, sPON_ME2 did not show to be absorbing at 470 nm. The implication of the background not going to zero (6.093) is that there is still an unexplained contribution to the absorbtion at 470 nm, unrelated to sPON_ME2.

In order to further explore the possibility of sPON_ME-2 absorbing at 470 nm, the HSC period was analysed, where sPON_ME2 was shown to be non-absorbing at 470 nm with a partial slope of zero. On the other hand, BBOA_2 had a partial slope of 27.288 and bkgd a value of 2.527. This background value suggests there is another component related to b$_{abs}$ that is not sPON. Thus, a trilinear regression was performed to *HSC between babs and BBOA_2, sPON and LVOOA. Here, the background value drops to 1.649, sPON partial slope is zero and LVOOA presents a partial slope of 1.138. These results

390 confirm that sPON do not absorb light at 470 nm while LVOOA, or at least part of the components of LVOOA, absorb during the HSC event and pPON_ME2 absorbs during the bfo event.

These results agree with previous studies that found biomass burning OA contain important concentrations of light absorbing brown carbon (BrC) and that certain types of SOA are effective absorbers near UV light (Bones et al., 2010;Saleh et al., 2014). The fact that pPON_ME2 and LVOOA were shown to be absorbing light at a short wavelength (470 nm) will have a direct impact on Aethalometer model studies; while pPON_ME2 could be considered a component of the wood burning

395 aerosol apportioned using the Aethalometer, it may be that there is an interference from other forms of BrC in SOA. However, this work would suggest that sPON specifically does not contribute to the latter, so a different component of LV-OOA would have to be responsible. As well as Aethalometer interpretation, it is also worth mentioning that these findings may have implications for studies on the radiative properties of the atmosphere, as BrC is also thought to affect climate (Jacobson, 2014).

400 5. Conclusions

In order to better understand the aerosol chemical composition and variation in source contribution during periods of nocturnal pollution, online measurements of gases and aerosols were made in ambient air between 29th October and 10th November 2014, at the University of Manchester with detailed analysis of the special high pollutant concentrations during bonfire night celebrations on 5th November. High aerosol concentrations were observed during the bonfire night event with

405 115 $\mu g.m^{-3}$ of PM_1. Important nitrogen chemistry was present with high HCN, HCNO and HONO concentrations primarily emitted with further presence of N_2O_5 and $ClNO_2$ concentrations from nocturnal nitrate chemistry taking place after NO_x concentrations decreased.

Organic aerosol source apportionment was successfully applied, using the ME-2 factorisation tool, during the bonfire night. The particular high pollutant concentrations together with the complex mix of emissions did not allow the running of ME-2

410 for the complete dataset, thus the dataset was divided into different periods. The best way to perform source apportionment was found to be to, (a) analyse the period before and after the bonfire night using BBOA, HOA and COA from a previous study in Paris as TP, and (b) conduct a further ME-2 analysis of the bonfire night period using BBOA, HOA and COA mass spectra from (a) as TP. Moreover, an improvement on the source apportionment was observed after modifying the fragPanel in order to identify organic nitrate sources, increasing the r^2 value from linear regressions between b_{abs_470wb} (absorption

415 coefficient of wood burning at 470 nm) and BBOA from 0.839 to 0.880.

The combination of CIMS measurements and OA sources determined from AMS measurements provided important information about gas tracers to be used as inputs (target time series) to improve future ME-2 analyses, particularly gases correlating with BBOA, LVOOA and secondary particulate organic nitrate. However the use of these species as target time series should be used with care as their time variation are greatly affected by meteorological conditions.

420 The presence of two classes of particulate organic nitrate (PON), secondary (sPON_ME2) and primary (pPON_ME2) PON, was identified both from looking at the BBOA:PON relationship and from the ME-2 analysis after modifying the FragPanel. It is clear that, during bonfire night, pPON_ME2 concentrations increased when BBOA concentrations are present and sPON_ME2 concentrations started evolving when the primary concentrations decreased.

It was determined that pPON_ME2 absorbed light at a wavelenght of 470 nm during the bonfire night, where the multilinear

425 regression perfomed between b_{abs_470wb}, BBOA and pPON_ME2 showed a high r^2 of 0.910 while sPON_ME2 did not contribute to light absorption at 470nm. During the HSC episode, LVOOA showed a partial slope of 1.138 in the multilinear

regression and an r^2 from linear regression with b_{abs_470wb} of 0.225, implying secondary LVOOA (associated with SOA) may be absorbing at 470 nm and sPON_ME2 was not absorbing at this wavelength. These results will help us to understand the mechanistic contributions to UV absorption in the Aethalometer and will have direct implications for source apportionment
430 studies, which may need to be corrected for secondary organic aerosol interferences near the UV region.

6. Data availability

Processed data is available through the archive at the British Atmospheric Data Centre (http://badc.nerc.ac.uk/browse/badc), with search term `COMPART'. Raw data is archived at the University of Manchester and is available on request.

Author contributions. Ernesto Reyes-Villegas, Michael Flynn, Hugh Coe, Carl Percival, James Allan designed the project;
435 Ernesto Reyes-Villegas, Yu-Chieh Ting, Sophie Haslett, Thomas Bannan, Michael Le breton, Paul Williams, Asan Bacak, operated, calibrated and performed QA of instrument measurements; Ernesto Reyes-Villegas and Michael Priestley performed the data analysis; Ernesto Reyes-Villegas, Hugh Coe and James Allan wrote the paper.

Acknowledgements. This work was supported through the UK Natural Environment Research Council (NERC) through the Com-Part (grant ref: NE/K014838/1). Ernesto Reyes-Villegas is supported by a studentship by the National Council of
440 Science and Technology-Mexico (CONACYT) under registry number 217687.

References

Ainsworth, W. H.: Guy fawkes; or, the gunpowder treason, Nottingham Society, 1850.
Alfarra, M. R., Paulsen, D., Gysel, M., Garforth, A. A., Dommen, J., Prévôt, A. S. H., Worsnop, D. R., Baltensperger, U., and Coe, H.: A mass spectrometric study of secondary organic aerosols formed from the
445 photooxidation of anthropogenic and biogenic precursors in a reaction chamber, Atmos Chem Phys, 6, 5279-5293, 2006.
Allan, J. D., Delia, A. E., Coe, H., Bower, K. N., Alfarra, M. R., Jimenez, J. L., Middlebrook, A. M., Drewnick, F., Onasch, T. B., Canagaratna, M. R., Jayne, J. T., and Worsnop, D. R.: A generalised method for the extraction of chemically resolved mass spectra from aerodyne aerosol mass spectrometer data, J Aerosol Sci, 35, 909-922,
450 DOI 10.1016/j.jaerosci.2004.02.007, 2004.
Allan, J. D., Alfarra, M. R., Bower, K. N., Coe, H., Jayne, J. T., Worsnop, D. R., Aalto, P. P., Kulmala, M., Hyötyläinen, T., Cavalli, F., and Laaksonen, A.: Size and composition measurements of background aerosol and new particle growth in a finnish forest during quest 2 using an aerodyne aerosol mass spectrometer, Atmos. Chem. Phys., 6, 315-327, 10.5194/acp-6-315-2006, 2006.
455 Ayres, B. R., Allen, H. M., Draper, D. C., Brown, S. S., Wild, R. J., Jimenez, J. L., Day, D. A., Campuzano-Jost, P., Hu, W., de Gouw, J., Koss, A., Cohen, R. C., Duffey, K. C., Romer, P., Baumann, K., Edgerton, E., Takahama, S., Thornton, J. A., Lee, B. H., Lopez-Hilfiker, F. D., Mohr, C., Wennberg, P. O., Nguyen, T. B., Teng, A., Goldstein, A. H., Olson, K., and Fry, J. L.: Organic nitrate aerosol formation via no3 + biogenic volatile organic compounds in the southeastern united states, Atmos. Chem. Phys., 15, 13377-13392, 10.5194/acp-15-13377-2015, 2015.
460 Bannan, T. J., Booth, A. M., Bacak, A., Muller, J. B. A., Leather, K. E., Le Breton, M., Jones, B., Young, D., Coe, H., Allan, J., Visser, S., Slowik, J. G., Furger, M., Prevot, A. S. H., Lee, J., Dunmore, R. E., Hopkins, J. R., Hamilton, J. F., Lewis, A. C., Whalley, L. K., Sharp, T., Stone, D., Heard, D. E., Fleming, Z. L., Leigh, R., Shallcross, D. E., and Percival, C. J.: The first uk measurements of nitryl chloride using a chemical ionization mass spectrometer in central london in the summer of 2012, and an investigation of the role of cl atom oxidation, J Geophys Res-
465 Atmos, 120, 5638-5657, 10.1002/2014JD022629, 2015.
Bones, D. L., Henricksen, D. K., Mang, S. A., Gonsior, M., Bateman, A. P., Nguyen, T. B., Cooper, W. J., and Nizkorodov, S. A.: Appearance of strong absorbers and fluorophores in limonene-o3 secondary organic aerosol due to nh4+-mediated chemical aging over long time scales, Journal of Geophysical Research: Atmospheres, 115, n/a-n/a, 10.1029/2009jd012864, 2010.

470 Bruns, E. A., Perraud, V., Zelenyuk, A., Ezell, M. J., Johnson, S. N., Yu, Y., Imre, D., Finlayson-Pitts, B. J., and Alexander, M. L.: Comparison of ftir and particle mass spectrometry for the measurement of particulate organic nitrates, Environmental Science & Technology, 44, 1056-1061, 10.1021/es9029864, 2010.

Canonaco, F., Crippa, M., Slowik, J. G., Baltensperger, U., and Prevot, A. S. H.: Sofi, an igor-based interface for the efficient use of the generalized multilinear engine (me-2) for the source apportionment: Me-2 application to

475 aerosol mass spectrometer data, Atmos Meas Tech, 6, 3649-3661, DOI 10.5194/amt-6-3649-2013, 2013.

Chakraborty, A., Gupta, T., and Tripathi, S. N.: Chemical composition and characteristics of ambient aerosols and rainwater residues during indian summer monsoon: Insight from aerosol mass spectrometry, Atmos Environ, 136, 144-155, 10.1016/j.atmosenv.2016.04.024, 2016.

Clark, H.: New directions. Light blue touch paper and retire, Atmos Environ, 31, 2893-2894, 10.1016/s1352-

480 2310(97)88278-7, 1997.

Colbeck, I., and Chung, M.-C.: Ambient aerosol concentrations at a site in se england during bonfire night 1995, J Aerosol Sci, 27, Supplement 1, S449-S450, http://dx.doi.org/10.1016/0021-8502(96)00297-2, 1996.

Crilley, L. R., Bloss, W. J., Yin, J., Beddows, D. C. S., Harrison, R. M., Allan, J. D., Young, D. E., Flynn, M., Williams, P., Zotter, P., Prevot, A. S. H., Heal, M. R., Barlow, J. F., Halios, C. H., Lee, J. D., Szidat, S., and Mohr, C.: Sources

485 and contributions of wood smoke during winter in london: Assessing local and regional influences, Atmos. Chem. Phys., 15, 3149-3171, 10.5194/acp-15-3149-2015, 2015.

Crippa, M., DeCarlo, P. F., Slowik, J. G., Mohr, C., Heringa, M. F., Chirico, R., Poulain, L., Freutel, F., Sciare, J., Cozic, J., Di Marco, C. F., Elsasser, M., Nicolas, J. B., Marchand, N., Abidi, E., Wiedensohler, A., Drewnick, F., Schneider, J., Borrmann, S., Nemitz, E., Zimmermann, R., Jaffrezo, J. L., Prevot, A. S. H., and Baltensperger, U.:

490 Wintertime aerosol chemical composition and source apportionment of the organic fraction in the metropolitan area of paris, Atmos Chem Phys, 13, 961-981, DOI 10.5194/acp-13-961-2013, 2013.

Crippa, M., Canonaco, F., Lanz, V. A., Aijala, M., Allan, J. D., Carbone, S., Capes, G., Ceburnis, D., Dall'Osto, M., Day, D. A., DeCarlo, P. F., Ehn, M., Eriksson, A., Freney, E., Ruiz, L. H., Hillamo, R., Jimenez, J. L., Junninen, H., Kiendler-Scharr, A., Kortelainen, A. M., Kulmala, M., Laaksonen, A., Mensah, A., Mohr, C., Nemitz, E., O'Dowd,

495 C., Ovadnevaite, J., Pandis, S. N., Petaja, T., Poulain, L., Saarikoski, S., Sellegri, K., Swietlicki, E., Tiitta, P., Worsnop, D. R., Baltensperger, U., and Prevot, A. S. H.: Organic aerosol components derived from 25 ams data sets across europe using a consistent me-2 based source apportionment approach, Atmos Chem Phys, 14, 6159-6176, DOI 10.5194/acp-14-6159-2014, 2014.

Day, D. A., Liu, S., Russell, L. M., and Ziemann, P. J.: Organonitrate group concentrations in submicron particles

500 with high nitrate and organic fractions in coastal southern california, Atmos Environ, 44, 1970-1979, http://dx.doi.org/10.1016/j.atmosenv.2010.02.045, 2010.

Drewnick, F., Hings, S. S., DeCarlo, P., Jayne, J. T., Gonin, M., Fuhrer, K., Weimer, S., Jimenez, J. L., Demerjian, K. L., Borrmann, S., and Worsnop, D. R.: A new time-of-flight aerosol mass spectrometer (tof-ams) - instrument description and first field deployment, Aerosol Science and Technology, 39, 637-658, Doi

505 10.1080/02786820500182040, 2005.

Drewnick, F., Hings, S. S., Curtius, J., Eerdekens, G., and Williams, J.: Measurement of fine particulate and gas-phase species during the new year's fireworks 2005 in mainz, germany, Atmos Environ, 40, 4316-4327, http://dx.doi.org/10.1016/j.atmosenv.2006.03.040, 2006.

Drewnick, F., Diesch, J. M., Faber, P., and Borrmann, S.: Aerosol mass spectrometry: Particle–vaporizer

510 interactions and their consequences for the measurements, Atmos. Meas. Tech., 8, 3811-3830, 10.5194/amt-8-3811-2015, 2015.

Dyke, P., Coleman, P., and James, R.: Dioxins in ambient air, bonfire night 1994, Chemosphere, 34, 1191-1201, http://dx.doi.org/10.1016/S0045-6535(97)00418-9, 1997.

EEA: Status of black carbon monitoring in ambient air in europe, 48, 2013.

515 Faber, P., Drewnick, F., Veres, P. R., Williams, J., and Borrmann, S.: Anthropogenic sources of aerosol particles in a football stadium: Real-time characterization of emissions from cigarette smoking, cooking, hand flares, and color smoke bombs by high-resolution aerosol mass spectrometry, Atmos Environ, 77, 1043-1051, DOI 10.1016/j.atmosenv.2013.05.072, 2013.

Farmer, D. K., Matsunaga, A., Docherty, K. S., Surratt, J. D., Seinfeld, J. H., Ziemann, P. J., and Jimenez, J. L.:

520 Response of an aerosol mass spectrometer to organonitrates and organosulfates and implications for atmospheric chemistry, Proceedings of the National Academy of Sciences of the United States of America, 107, 6670-6675, 10.1073/pnas.0912340107, 2010.

Farrar, N. J., Smith, K. E. C., Lee, R. G. M., Thomas, G. O., Sweetman, A. J., and Jones, K. C.: Atmospheric emissions of polybrominated diphenyl ethers and other persistent organic pollutants during a major

525   anthropogenic combustion event, Environmental Science & Technology, 38, 1681-1685, 10.1021/es035127d, 2004.

Fernandez, P., Grifoll, M., Solanas, A. M., Bayona, J. M., and Albaiges, J.: Bioassay-directed chemical analysis of genotoxic components in coastal sediments, Environmental Science & Technology, 26, 817-829, 10.1021/es00028a024, 1992.

530   Flowers, B. A., Dubey, M. K., Mazzoleni, C., Stone, E. A., Schauer, J. J., Kim, S. W., and Yoon, S. C.: Optical-chemical-microphysical relationships and closure studies for mixed carbonaceous aerosols observed at jeju island; 3-laser photoacoustic spectrometer, particle sizing, and filter analysis, Atmos. Chem. Phys., 10, 10387-10398, 10.5194/acp-10-10387-2010, 2010.

Frohlich, R., Crenn, V., Setyan, A., Belis, C. A., Canonaco, F., Favez, O., Riffault, V., Slowik, J. G., Aas, W., Aijala,
535   M., Alastuey, A., Artinano, B., Bonnaire, N., Bozzetti, C., Bressi, M., Carbone, C., Coz, E., Croteau, P. L., Cubison, M. J., Esser-Gietl, J. K., Green, D. C., Gros, V., Heikkinen, L., Herrmann, H., Jayne, J. T., Lunder, C. R., Minguillon, M. C., Mocnik, G., O'Dowd, C. D., Ovadnevaite, J., Petralia, E., Poulain, L., Priestman, M., Ripoll, A., Sarda-Esteve, R., Wiedensohler, A., Baltensperger, U., Sciare, J., and Prevot, A. S. H.: Actris acsm intercomparison - part 2: Intercomparison of me-2 organic source apportionment results from 15 individual, co-located aerosol mass
540   spectrometers, Atmos Meas Tech, 8, 2555-2576, 10.5194/amt-8-2555-2015, 2015.

Fry, J. L., Kiendler-Scharr, A., Rollins, A. W., Wooldridge, P. J., Brown, S. S., Fuchs, H., Dubé, W., Mensah, A., dal Maso, M., Tillmann, R., Dorn, H. P., Brauers, T., and Cohen, R. C.: Organic nitrate and secondary organic aerosol yield from no3 oxidation of β-pinene evaluated using a gas-phase kinetics/aerosol partitioning model, Atmos. Chem. Phys., 9, 1431-1449, 10.5194/acp-9-1431-2009, 2009.

545   Godri, K. J., Green, D. C., Fuller, G. W., Dall'Osto, M., Beddows, D. C., Kelly, F. J., Harrison, R. M., and Mudway, I. S.: Particulate oxidative burden associated with firework activity, Environmental Science & Technology, 44, 8295-8301, 10.1021/es1016284, 2010.

Hamad, S., Green, D., and Heo, J.: Evaluation of health risk associated with fireworks activity at central london, Air Quality, Atmosphere & Health, 1-7, 10.1007/s11869-015-0384-x, 2015.

550   Hao, L. Q., Kortelainen, A., Romakkaniemi, S., Portin, H., Jaatinen, A., Leskinen, A., Komppula, M., Miettinen, P., Sueper, D., Pajunoja, A., Smith, J. N., Lehtinen, K. E. J., Worsnop, D. R., Laaksonen, A., and Virtanen, A.: Atmospheric submicron aerosol composition and particulate organic nitrate formation in a boreal forestland-urban mixed region, Atmos Chem Phys, 14, 13483-13495, 10.5194/acp-14-13483-2014, 2014.

Harrison, M. A. J., Barra, S., Borghesi, D., Vione, D., Arsene, C., and Iulian Olariu, R.: Nitrated phenols in the
555   atmosphere: A review, Atmos Environ, 39, 231-248, http://dx.doi.org/10.1016/j.atmosenv.2004.09.044, 2005.

Harrison, R. M., Beddows, D. C. S., Hu, L., and Yin, J.: Comparison of methods for evaluation of wood smoke and estimation of uk ambient concentrations, Atmos Chem Phys, 12, 8271-8283, DOI 10.5194/acp-12-8271-2012, 2012.

Jacobson, M. Z.: Isolating nitrated and aromatic aerosols and nitrated aromatic gases as sources of ultraviolet
560   light absorption, J Geophys Res-Atmos, 104, 3527-3542, Doi 10.1029/1998jd100054, 1999.

Jacobson, M. Z.: Effects of biomass burning on climate, accounting for heat and moisture fluxes, black and brown carbon, and cloud absorption effects, Journal of Geophysical Research: Atmospheres, 119, 8980-9002, 10.1002/2014jd021861, 2014.

Joshi, M., Khan, A., Anand, S., and Sapra, B. K.: Size evolution of ultrafine particles: Differential signatures of
565   normal and episodic events, Environmental Pollution, 208, Part B, 354-360, http://dx.doi.org/10.1016/j.envpol.2015.10.001, 2016.

Kiendler-Scharr, A., Mensah, A. A., Friese, E., Topping, D., Nemitz, E., Prevot, A. S. H., Äijälä, M., Allan, J., Canonaco, F., Canagaratna, M., Carbone, S., Crippa, M., Dall Osto, M., Day, D. A., De Carlo, P., Di Marco, C. F., Elbern, H., Eriksson, A., Freney, E., Hao, L., Herrmann, H., Hildebrandt, L., Hillamo, R., Jimenez, J. L., Laaksonen,
570   A., McFiggans, G., Mohr, C., O'Dowd, C., Otjes, R., Ovadnevaite, J., Pandis, S. N., Poulain, L., Schlag, P., Sellegri, K., Swietlicki, E., Tiitta, P., Vermeulen, A., Wahner, A., Worsnop, D., and Wu, H. C.: Ubiquity of organic nitrates from nighttime chemistry in the european submicron aerosol, Geophys Res Lett, 43, 7735-7744, 10.1002/2016gl069239, 2016.

Kitanovski, Z., Grgic, I., Vermeylen, R., Claeys, M., and Maenhaut, W.: Liquid chromatography tandem mass
575   spectrometry method for characterization of monoaromatic nitro-compounds in atmospheric particulate matter, J Chromatogr A, 1268, 35-43, 10.1016/j.chroma.2012.10.021, 2012.

LASKAR, S. I., JASWAL, K., BHATNAGAR, M. K., and RATHORE, L. S.: India meteorological department, India, 1021-1037, 2016.

580   Le Breton, M., Bacak, A., Muller, J. B. A., O'Shea, S. J., Xiao, P., Ashfold, M. N. R., Cooke, M. C., Batt, R., Shallcross, D. E., Oram, D. E., Forster, G., Bauguitte, S. J. B., Palmer, P. I., Parrington, M., Lewis, A. C., Lee, J. D., and Percival, C. J.: Airborne hydrogen cyanide measurements using a chemical ionisation mass spectrometer for the plume identification of biomass burning forest fires, Atmos. Chem. Phys., 13, 9217-9232, 10.5194/acp-13-9217-2013, 2013.

585   Le Breton, M., Bacak, A., Muller, J. B. A., Bannan, T. J., Kennedy, O., Ouyang, B., Xiao, P., Bauguitte, S. J. B., Shallcross, D. E., Jones, R. L., Daniels, M. J. S., Ball, S. M., and Percival, C. J.: The first airborne comparison of n2o5 measurements over the uk using a cims and bbceas during the ronoco campaign, Anal Methods-Uk, 6, 9731-9743, 10.1039/c4ay02273d, 2014a.

      Le Breton, M., Bacak, A., Muller, J. B. A., Xiao, P., Shallcross, B. M. A., Batt, R., Cooke, M. C., Shallcross, D. E., Bauguitte, S. J. B., and Percival, C. J.: Simultaneous airborne nitric acid and formic acid measurements using a
590   chemical ionization mass spectrometer around the uk: Analysis of primary and secondary production pathways, Atmos Environ, 83, 166-175, http://dx.doi.org/10.1016/j.atmosenv.2013.10.008, 2014b.

      Lee, B. H., Lopez-Hilfiker, F. D., Mohr, C., Kurtén, T., Worsnop, D. R., and Thornton, J. A.: An iodide-adduct high-resolution time-of-flight chemical-ionization mass spectrometer: Application to atmospheric inorganic and organic compounds, Environmental Science & Technology, 48, 6309-6317, 10.1021/es500362a, 2014.

595   Lee Ng, N., Brown, S. S., Archibald, A. T., Atlas, E., Cohen, R. C., Crowley, J. N., Day, D. A., Donahue, N. M., Fry, J. L., Fuchs, H., Griffin, R. J., Guzman, M. I., Herrmann, H., Hodzic, A., Iinuma, Y., Kiendler-Scharr, A., Lee, B. H., Luecken, D. J., Mao, J., McLaren, R., Mutzel, A., Osthoff, H. D., Ouyang, B., Picquet-Varrault, B., Platt, U., Pye, H. O. T., Rudich, Y., Schwantes, R. H., Shiraiwa, M., Stutz, J., Thornton, J. A., Tilgner, A., Williams, B. J., and Zaveri, R. A.: Nitrate radicals and biogenic volatile organic compounds: Oxidation, mechanisms, and organic aerosol,
600   Atmos Chem Phys, 17, 2103-2162, 10.5194/acp-17-2103-2017, 2017.

      Liu, D., Whitehead, J., Alfarra, M. R., Reyes-Villegas, E., Spracklen, D. V., Reddington, C. L., Kong, S., Williams, P. I., Ting, Y.-C., Haslett, S., Taylor, J. W., Flynn, M. J., Morgan, W. T., McFiggans, G., Coe, H., and Allan, J. D.: Black-carbon absorption enhancement in the atmosphere determined by particle mixing state, Nature Geosci, 10, 184-188, 10.1038/ngeo2901, 2017.

605   Mao, J., Paulot, F., Jacob, D. J., Cohen, R. C., Crounse, J. D., Wennberg, P. O., Keller, C. A., Hudman, R. C., Barkley, M. P., and Horowitz, L. W.: Ozone and organic nitrates over the eastern united states: Sensitivity to isoprene chemistry, Journal of Geophysical Research Atmosphers, 118, 11256-11268, 10.1002/jgrd.50817, 2013.

      Mohr, C., Lopez-Hilfiker, F. D., Zotter, P., Prevot, A. S. H., Xu, L., Ng, N. L., Herndon, S. C., Williams, L. R., Franklin,
610   J. P., Zahniser, M. S., Worsnop, D. R., Knighton, W. B., Aiken, A. C., Gorkowski, K. J., Dubey, M. K., Allan, J. D., and Thornton, J. A.: Contribution of nitrated phenols to wood burning brown carbon light absorption in detling, united kingdom during winter time, Environmental Science & Technology, 47, 6316-6324, Doi 10.1021/Es400683v, 2013.

      Moreno, T., Querol, X., Alastuey, A., Cruz Minguillón, M., Pey, J., Rodriguez, S., Vicente Miró, J., Felis, C., and
615   Gibbons, W.: Recreational atmospheric pollution episodes: Inhalable metalliferous particles from firework displays, Atmos Environ, 41, 913-922, http://dx.doi.org/10.1016/j.atmosenv.2006.09.019, 2007.

      Naeher, L. P., Brauer, M., Lipsett, M., Zelikoff, J. T., Simpson, C. D., Koenig, J. Q., and Smith, K. R.: Woodsmoke health effects: A review, Inhalation Toxicology, 19, 67-106, 10.1080/08958370600985875, 2007.

      Paatero, P., and Tapper, U.: Positive matrix factorization: A non-negative factor model with optimal utilization of
620   error estimates of data values, Environmetrics, 5, 111-126, 1994.

      Paatero, P.: The multilinear engine: A table-driven, least squares program for solving multilinear problems, including the n-way parallel factor analysis model, J Comput Graph Stat, 8, 854-888, 10.2307/1390831, 1999.

      Paglione, M., Kiendler-Scharr, A., Mensah, A. A., Finessi, E., Giulianelli, L., Sandrini, S., Facchini, M. C., Fuzzi, S., Schlag, P., Piazzalunga, A., Tagliavini, E., Henzing, J. S., and Decesari, S.: Identification of humic-like substances
625   (hulis) in oxygenated organic aerosols using nmr and ams factor analyses and liquid chromatographic techniques, Atmos Chem Phys, 14, 25-45, DOI 10.5194/acp-14-25-2014, 2014.

      Perring, A. E., Pusede, S. E., and Cohen, R. C.: An observational perspective on the atmospheric impacts of alkyl and multifunctional nitrates on ozone and secondary organic aerosol, Chemical Reviews, 113, 5848-5870, 10.1021/cr300520x, 2013.

630   Pervez, S., Chakrabarty, R. K., Dewangan, S., Watson, J. G., Chow, J. C., and Matawle, J. L.: Chemical speciation of aerosols and air quality degradation during the festival of lights (diwali), Atmospheric Pollution Research, 7, 92-99, 10.1016/j.apr.2015.09.002, 2016.

Petzold, A., Kramer, H., and Schonlinner, M.: Continuous measurement of atmospheric black carbon using a multi-angle absorption photometer, Environ Sci Pollut R, 78-82, 2002.

635 Priestley, M., Le Breton, M., Bannan, T. J., Leather, K. E., Bacak, A., Allan, J. D., Brazier, T., Reyes-Villegas, E., Shallcross, B. M. A., Khan, M. A., De Vocht, F., D.E., S., Coe, H., and Percival, C. J.: Manchester, uk bonfire night 2014: Air quality and emission ratios during an anthropogenic biomass burning event using a time of flight chemical ionisation mass spectrometer, In preparation.

Qingguo, H., Liansheng, W., and Shuokui, H.: The genotoxicity of substituted nitrobenzenes and the quantitative
640 structure-activity relationship studies, Chemosphere, 30, 915-923, 10.1016/0045-6535(94)00450-9, 1995.

Ravindra, K., Mor, S., and Kaushik, C. P.: Short-term variation in air quality associated with firework events: A case study, Journal of Environmental Monitoring, 5, 260-264, 10.1039/b211943a, 2003.

Reyes-Villegas, E., Green, D. C., Priestman, M., Canonaco, F., Coe, H., Prévôt, A. S. H., and Allan, J. D.: Organic aerosol source apportionment in london 2013 with me-2: Exploring the solution space with annual and seasonal
645 analysis, Atmos. Chem. Phys., 16, 15545-15559, 10.5194/acp-16-15545-2016, 2016.

Saleh, R., Robinson, E. S., Tkacik, D. S., Ahern, A. T., Liu, S., Aiken, A. C., Sullivan, R. C., Presto, A. A., Dubey, M. K., Yokelson, R. J., Donahue, N. M., and Robinson, A. L.: Brownness of organics in aerosols from biomass burning linked to their black carbon content, Nat Geosci, 7, 647-650, 10.1038/NGEO2220, 2014.

Sandradewi, J., Prévôt, A. S. H., Szidat, S., Perron, N., Alfarra, M. R., Lanz, V. A., Weingartner, E., and
650 Baltensperger, U. R. S.: Using aerosol light abosrption measurements for the quantitative determination of wood burning and traffic emission contribution to particulate matter, Environmental Science and Technology, 42, 3316-3323, 10.1021/es702253m, 2008.

Sato, K., Takami, A., Isozaki, T., Hikida, T., Shimono, A., and Imamura, T.: Mass spectrometric study of secondary organic aerosol formed from the photo-oxidation of aromatic hydrocarbons, Atmos Environ, 44, 1080-1087,
655 10.1016/j.atmosenv.2009.12.013, 2010.

Teich, M., van Pinxteren, D., Wang, M., Kecorius, S., Wang, Z., Müller, T., Močnik, G., and Herrmann, H.: Contributions of nitrated aromatic compounds to the light absorption of water-soluble and particulate brown carbon in different atmospheric environments in germany and china, Atmos. Chem. Phys., 17, 1653-1672, 10.5194/acp-17-1653-2017, 2017.

660 Tian, Y. Z., Wang, J., Peng, X., Shi, G. L., and Feng, Y. C.: Estimation of the direct and indirect impacts of fireworks on the physicochemical characteristics of atmospheric pm10 and pm2.5, Atmos Chem Phys, 14, 9469-9479, 10.5194/acp-14-9469-2014, 2014.

Vassura, I., Venturini, E., Marchetti, S., Piazzalunga, A., Bernardi, E., Fermo, P., and Passarini, F.: Markers and influence of open biomass burning on atmospheric particulate size and composition during a major bonfire
665 event, Atmos Environ, 82, 218-225, 10.1016/j.atmosenv.2013.10.037, 2014.

Vecchi, R., Bernardoni, V., Cricchio, D., D'Alessandro, A., Fermo, P., Lucarelli, F., Nava, S., Piazzalunga, A., and Valli, G.: The impact of fireworks on airborne particles, Atmos Environ, 42, 1121-1132, http://dx.doi.org/10.1016/j.atmosenv.2007.10.047, 2008.

Veres, P., Roberts, J. M., Burling, I. R., Warneke, C., de Gouw, J., and Yokelson, R. J.: Measurements of gas-phase
670 inorganic and organic acids from biomass fires by negative-ion proton-transfer chemical-ionization mass spectrometry, Journal of Geophysical Research: Atmospheres, 115, n/a-n/a, 10.1029/2010jd014033, 2010.

Visser, S., Slowik, J. G., Furger, M., Zotter, P., Bukowiecki, N., Canonaco, F., Flechsig, U., Appel, K., Green, D. C., Tremper, A. H., Young, D. E., Williams, P. I., Allan, J. D., Coe, H., Williams, L. R., Mohr, C., Xu, L., Ng, N. L., Nemitz, E., Barlow, J. F., Halios, C. H., Fleming, Z. L., Baltensperger, U., and Prévôt, A. S. H.: Advanced source
675 apportionment of size-resolved trace elements at multiple sites in london during winter, Atmos. Chem. Phys., 15, 11291-11309, 10.5194/acp-15-11291-2015, 2015.

Wang, L. W., Wen, L., Xu, C. H., Chen, J. M., Wang, X. F., Yang, L. X., Wang, W. X., Yang, X., Sui, X., Yao, L., and Zhang, Q. Z.: Hono and its potential source particulate nitrite at an urban site in north china during the cold season, Science of The Total Environment, 538, 93-101, 10.1016/j.scitotenv.2015.08.032, 2015.

680 Wang, Y., Zhuang, G., Xu, C., and An, Z.: The air pollution caused by the burning of fireworks during the lantern festival in beijing, Atmos Environ, 41, 417-431, http://dx.doi.org/10.1016/j.atmosenv.2006.07.043, 2007.

Weingartner, E., Saathoff, H., Schnaiter, M., Streit, N., Bitnar, B., and Baltensperger, U.: Absorption of light by soot particles: Determination of the absorption coefficient by means of aethalometers, J Aerosol Sci, 34, 1445-1463, 10.1016/S0021-8502(03)00359-8, 2003.

685 Young, D. E., Allan, J. D., Williams, P. I., Green, D. C., Harrison, R. M., Yin, J., Flynn, M. J., Gallagher, M. W., and Coe, H.: Investigating a two-component model of solid fuel organic aerosol in london: Processes, pm1 contributions, and seasonality, Atmos Chem Phys, 15, 2429-2443, 10.5194/acp-15-2429-2015, 2015.

Yuan, B., Liggio, J., Wentzell, J., Li, S. M., Stark, H., Roberts, J. M., Gilman, J., Lerner, B., Warneke, C., Li, R., Leithead, A., Osthoff, H. D., Wild, R., Brown, S. S., and de Gouw, J. A.: Secondary formation of nitrated phenols: Insights from observations during the uintah basin winter ozone study (ubwos) 2014, Atmos. Chem. Phys., 16, 2139-2153, 10.5194/acp-16-2139-2016, 2016.

Zhang, J. K., Cheng, M. T., Ji, D. S., Liu, Z. R., Hu, B., Sun, Y., and Wang, Y. S.: Characterization of submicron particles during biomass burning and coal combustion periods in beijing, china, Science of The Total Environment, 562, 812-821, 10.1016/j.scitotenv.2016.04.015, 2016.

Zhang, M., Wang, X., Chen, J., Cheng, T., Wang, T., Yang, X., Gong, Y., Geng, F., and Chen, C.: Physical characterization of aerosol particles during the chinese new year's firework events, Atmos Environ, 44, 5191-5198, http://dx.doi.org/10.1016/j.atmosenv.2010.08.048, 2010.

Zotter, P., Herich, H., Gysel, M., El-Haddad, I., Zhang, Y., Močnik, G., Hüglin, C., Baltensperger, U., Szidat, S., and Prévôt, A. S. H.: Evaluation of the absorption ångström exponents for traffic and wood burning in the aethalometer-based source apportionment using radiocarbon measurements of ambient aerosol, Atmos. Chem. Phys., 17, 4229-4249, 10.5194/acp-17-4229-2017, 2017.

Appendix A: Symbols and description of main parameters used.

Symbol	Name
	Periods of analysis
bfo	bonfire-only period (November 05-17:00 hrs – 06 - 12:00 hrs)
nbf	not bonfire (before and after bonfire night)
HSC	High secondary concentrations (October 30th to November 1st)
LC	Low concentrations (November 1st - 3rd)
WL	Winter-like (November 8th -10th)
	Aethalometer correction and model
α	Ångström absorption exponent
α_{tr}	Ångström absorption exponent for traffic
α_{wb}	Ångström absorption exponent for wood burning
ATN	Atennuation
BC	black carbon [µg.m^{-3}]
b_{abs}	absorption coefficient [m^{-1}]
b_{abs_470}	absorption coefficient at 470 nm [m^{-1}]
b_{abs_950}	absorption coefficient at 950 nm [m^{-1}]
σ_{ATN}	attenuation cross section [m^2.g^{-1}]
λ	wavelength [nm]
b_{ATN}	Uncorrected absorption coefficient [Mm^{-1}]
b_{abs}	Corrected absorption coefficient [Mm^{-1}]
C	Multiple scattering correction constant
R	Filter loading correction
f	shadowing factor
	Organic aerosol factors (OA)
BBOA	Biomass burning organic OA obtained without modifying the fragmentation table
BBOA_1	Second biomass burning organic OA obtained without modifying the fragmentation table
BBOA_2	biomass burning organic OA obtained after modifying the fragmentation table
HOA	Hydrocarbon-like OA
COA	Cooking OA
SVOOA	Semivolatile OA
LVOOA	Low volatility OA

PON	Particulate organic nitrate, calculated with 46:30 ratios.
pPON	Primary particulate organic nitrate, estimated using the slope between PON and BBOA
sPON	Secondary particulate organic nitrate, sPON = PON - pPON
pPON_ME2	Primary particulate organic nitrate, calculated from ME-2 analysis
sPON_ME2	Secondary particulate organic nitrate, calculated from ME-2 analysis

705
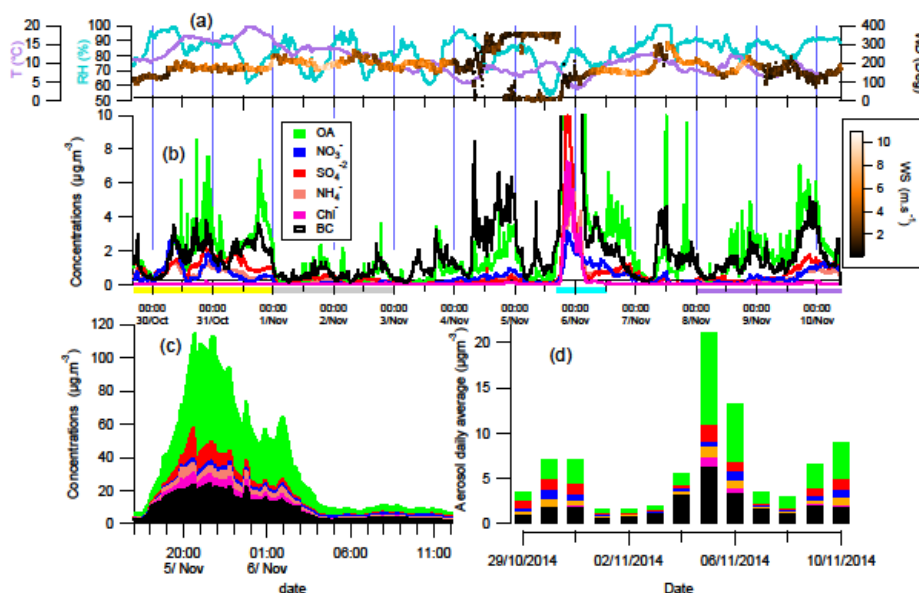
Figure 1: Meteorology (a), aerosol concentrations during all measurement period (b). Chemical component mass concentrations during bonfire night plotted cumulatively (c). Daily aerosol concentrations (d).

710
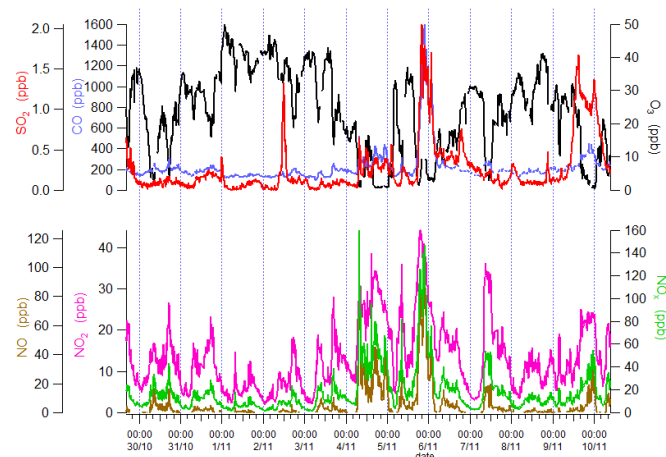
Figure 2: Time series of gases measured at Whitworth observatory.
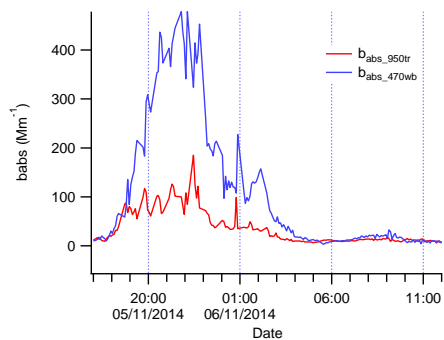
Figure 3: Absorption coefficients for Wood burning (wb) and traffic (tr).

715
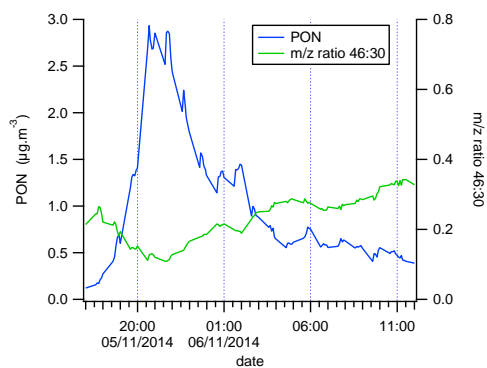
Figure 4: PON concentrations during bonfire night.
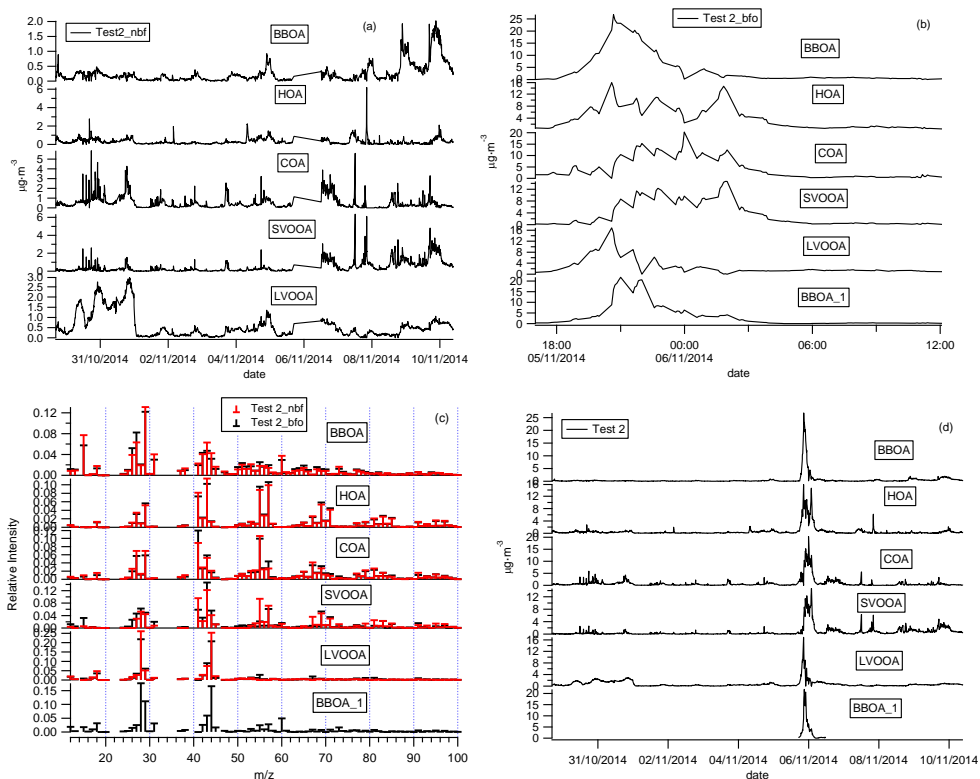
720

Figure 5: OA sources mass spectra and time series for test 2.
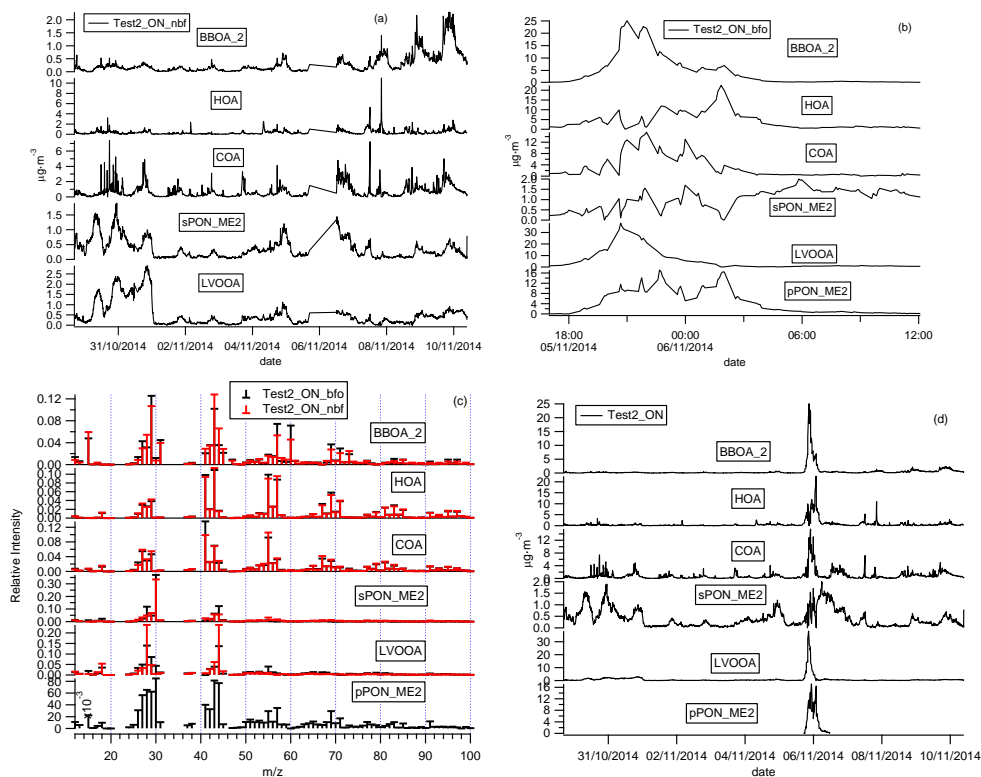
Figure 6: OA sources mass spectra and time series for test 2_ON.

725
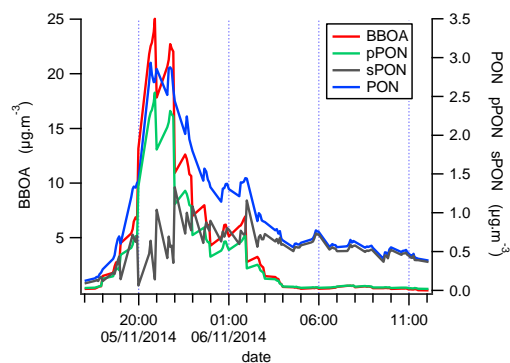
Figure 7: Secondary (sPON) and primary (pPON) organic nitrate time series estimated from PON and BBOA.
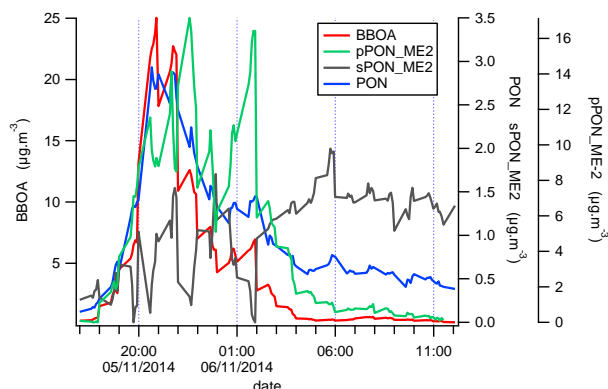
Figure 8: Secondary and primary organic nitrate time series obtained from ME-2 analysis.
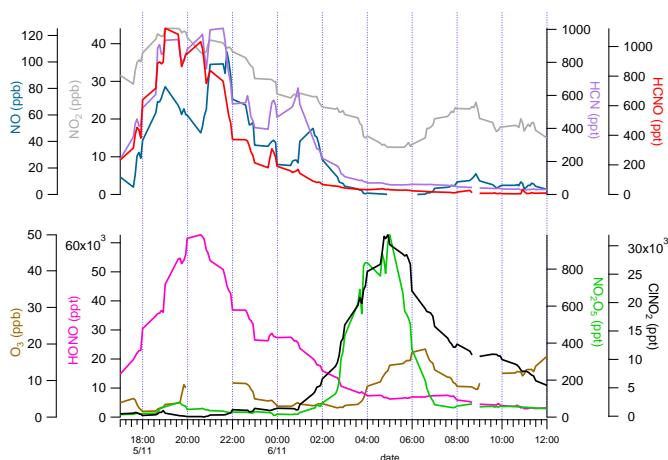
730   **Figure 9: Time series of gases pollutants during bonfire night.**

Table 1: Multilinear and linear regression analysis between babs_470wb and organic aerosols.

			All	HSC	LC	bfo	WL
MLR 1	A	bkgrd	0.000	3.037	0.999	0.000	1.117
	B	babs:BBOA	6.809	3.837	12.503	5.547	7.996
	C	babs:PON	34.865	8.384	8.267	43.592	12.780
		B/C	0.195	0.458	1.512	0.127	0.626
		r²_MLR	0.907	0.136	0.423	0.887	0.838
Linear 1	r²	babs:BBOA	0.848	0.095	0.416	0.830	0.824
	r²	babs:PON	0.823	0.125	0.319	0.875	0.313
MLR 2	A	bkgrd	0.055	1.802	0.836	0.000	0.260
	B	babs:BBOA_2	7.506	21.874	16.158	6.670	7.613
	C	babs:PON	28.876	0.000	4.459	34.809	11.463
		B/C	0.260	***	3.624	0.192	0.664
		r²_MLR	0.918	0.580	0.509	0.892	0.867
Linear 2	r²	babs:BBOA_2	0.885	0.580	0.506	0.871	0.855
	r²	babs:PON	0.823	0.125	0.319	0.875	0.313

			All	HSC	*HSC	LC	*bfo	WL
MLR 3	A	bkgrd	0.898	1.802	1.179	0.822	10.141	0.056
	B	babs:BBOA_2	11.267	21.874	18.662	15.945	8.769	6.754
	C	babs:sPON_ME2	3.840	0.000	0.000	1.690	0.000	5.927
	D	D			0.808		3.207	
		B/C	2.934	***	***	9.433	***	1.140
		B/D			23.099		2.734	
		r²_MLR	0.889	0.580	0.610	0.510	0.893	0.867
Linear 3	r²	babs:BBOA_2	0.885	0.580	0.580	0.506	0.871	0.855
	r²	babs:sPON_ME2	0.033	0.022	0.022	0.326	0.194	0.684
	r²	r²_D			0.312		0.600	

*Trilinear regression was performed as in *bfo analysis there were two PON factors from ME-2 analysis; pPON and sPON, with D= slope babs:pPON, r²_D = r² babs:pPON. In *HSC analysis; BBOA, sPON and LVOOA were used, with D= slope babs:LVOOA, r²_D = r² babs:LVOOA. PON is the particulate organic nitrate estimate from 46:30 ratios. All= complete
735   dataset; HSC= Episode with high secondary concentrations (October 30th to November 1st), LC = Episode with low concentrations (November 1st - 3rd); bfo = epidose with bonfire only concentrations (05-Nov 17:00 hrs – 06-Nov 12:00 hrs); WL= Episode with winter-like carachteristics (November 8th -10th).